AIMS Mathematics

https://www.aimspress.com/journal/Math

AIMS Mathematics, 11(7): 20085–20102.
DOI: 10.3934/math.2026816
Received: 15 April 2026
Revised: 26 June 2026
Accepted: 26 June 2026
Published: 08 July 2026

Research article

Embedding edge-disjoint Hamiltonian cycles in complete Josephus cubes with applications to fault-tolerant data broadcasting

Ying Gao[1], **Lantao You**[1] **and Yuejuan Han**[2,*]

[1] School of Information Engineering, Suzhou Industrial Park Institute of Services Outsourcing, Suzhou, Jiangsu 215000, China

[2] School of Computer Science and Technology, Soochow University, Suzhou, Jiangsu 215000, China

* **Correspondence:** Email:hyj@suda.edu.cn.

Abstract: Edge-disjoint Hamiltonian cycles, abbreviated as EDHCs, provide multiple edge-disjoint communication paths for data broadcasting, which greatly enhance the reliability and fault tolerance of data transmission. The complete Josephus cube CJC_n possesses many desirable properties as a typical interconnection network. In this paper, we focus on the construction of EDHCs in CJC_n. We prove that there exist two EDHCs in CJC_n when $n \geq 3$, and three EDHCs in CJC_n when $n \geq 4$.

Keywords: edge-disjoint; Hamiltonian cycle; complete Josephus cube; fault tolerance; interconnection network
Mathematics Subject Classification: 05C38, 05C45

1. Introduction

High-performance computers, or supercomputers, are designed to execute large-scale scientific and engineering computations. These systems integrate numerous processing nodes to solve complex problems that cannot be handled by traditional computers. Interconnection networks act as the communication backbone in high-performance computers. Fault tolerance is critically important in high-performance interconnection networks. As the scale of parallel computing systems continues to grow, the probability of node or link failures increases significantly.

A ring (or cycle) structure stands as a representative foundational structure in interconnection networks. It organizes network nodes into a closed circular connection pattern, offering simplicity, regularity, and strong structural symmetry. The ring supports reliable message transmission and offers simplicity in hardware implementation. A Hamiltonian cycle refers to a cycle (or ring) that traverses every node in a network precisely once and returns to the starting node. Edge-disjoint Hamiltonian cycles (EDHCs) are a set of Hamiltonian cycles that share no common edges with each other. In interconnection networks, such structures can provide multiple independent and parallel transmission paths for data broadcasting. This effectively mitigates the adverse impacts caused by the increased probability of node or link failures as the scale of parallel computing systems continues to expand.

Recently, numerous studies on EDHCs of hypercube variants and related networks were carried out. Bae and Bose [1] generated EDHCs in hypercubes via a coding theory approach. Huang showed that there respectively exist two EDHCs in an n-dimensional locally twisted cube LTQ_n [2], an n-dimensional augmented cube AQ_n [3], and an n-dimensional crossed cube CQ_n [4]. Pai [5] put forward two algorithms to construct two EDHCs within a shuffle-cube SQ_6, and additionally established recursive constructions of two EDHCs in SQ_n for any $n \geq 6$. Yang et al. [6] proved the existence of two EDHCs in a spined cube SQ_n for any integer $n \geq 4$. Based on the recursive structure of CQ_n, Pai et al. [7] proved by induction that three EDHCs exist in a crossed cube CQ_n for $n \geq 6$, and then evaluated the data broadcasting performance enabled by these three EDHCs. Pai also showed that there exist three EDHCs in LTQ_n [8], $FLTQ_n$ (the folded locally twisted cube) , and FCQ_n (the folded crossed cube) [9] for $n \geq 6$. Lv and Wu [10] demonstrated that two EDHCs exist in a balanced hypercube BH_n when $n \geq 2$. Later, Liu et al. [11] designed multiple construction schemes to obtain $2^{\lfloor \log_2 n \rfloor}$ EDHCs in BH_n for $n \geq 2$, and simulated fault-tolerant data broadcasting using these parallel cycles as transmission channels.

The n-dimensional hypercube [12] Q_n ($n \geq 1$) is a classic interconnection network topology with core advantages that make it a foundational choice for parallel and distributed systems. It is a vertex-transitive and edge-transitive graph with each node having a degree of n. Although capable of accommodating an extensive array of applications, the hypercube is afflicted by inadequate size scalability. The Josephus cube, introduced in [13], is a refined interconnection topology that enhances the topological characteristics of Q_n. In comparison with the hypercube, it exhibits better scalability, smaller diameter, and higher communication efficiency. However, when deployed as a node cluster, the Josephus cube compromises a certain level of fault tolerance to achieve incremental scalability. To enhance fault tolerance while preserving routing efficiency at the node cluster level, the complete Josephus cube (CJC_n) is introduced [13].

Recently, CJC_n has attracted significant attention. Huang et al. investigated the strongly Menger edge-connectedness of the CJC_n in [14] and studied the h-extra diagnosability of CJC_n under both the Preparata, Metze, and Chien (PMC) model and the Maeng and Malek (MM) model in [15]. He et al. proposed a parallel algorithm to construct $n + 2$ ($n \geq 4$) vertex-independent spanning trees in CJC_n using 2^n processors in [16], and presented a parallel algorithm to construct $n + 2$ edge-independent trees with $O(n)$ time complexity in [17]. Liu et al. [18] explored the reliability of the h-extra edge-connectivity $\lambda_h(CJC_n)$ of the complete Josephus cube. Yang et al. [19] introduced a unified method that employs the edge isoperimetric problem from combinatorial studies to rigorously examine the $\mathfrak{R}$-conditional edge-connectivities of CJC_n.

In this paper, our research mainly focuses on the EDHCs in complete Josephus cube networks. The key contributions of this study are outlined as follows:
(1) We theoretically prove the existence of two EDHCs in CJC_n networks for $n \geq 3$.
(2) We further demonstrate the existence of three EDHCs in CJC_n networks where $n \geq 4$.
(3) By using multiple Hamiltonian cycles for data transmission when faulty edges occur, we conduct experimental tests to evaluate the fault tolerance performance of CJC_n networks.

2. Preliminaries

We often model an interconnection network using an undirected graph $G = (V(G), E(G))$, where $V(G)$ corresponds to the set of processors in the network, and $E(G)$ represents the communication links between processors. In this work, the terminology "vertex" and "node" are employed interchangeably. Here, we give some notations and definitions, which will be used in the following.

In a graph G, an edge is an unordered pair of distinct vertices $(x, y) \in E(G)$ connecting x and y. A path P is defined as a finite sequence of distinct vertices $\langle x_0, x_1, x_2, ..., x_k\rangle$ with $(x_i, x_{i+1}) \in E(G)$ for $0 \leq i \leq k-1$, and its reversed path is denoted by $P_{rev} = \langle x_k, x_{k-1}, x_{k-2}, ..., x_0\rangle$. A path with $x_0 = x_k$ and $k \geq 3$ is a cycle. The length of a path equals the number of its edges. We use $start(P)$ and $end(P)$ to denote the start and end vertices of path P, respectively.

The notation $R \Longrightarrow S$ represents the concatenation of paths R and S, connecting $end(R)$ to $start(S)$. Paths are edge-disjoint if their edge sets are pairwise disjoint, i.e., $E(P_i) \cap E(P_j) = \emptyset$ for $i \neq j$. A Hamiltonian path visits every vertex exactly once, and edge-disjoint Hamiltonian paths, abbreviated as EDHPs, share no common edges.

It is common to denote a node in V with an n-bit binary string u, which is expressed as $x_n x_{n-1} \cdots x_1$, where each $x_i \in \{0, 1\}$ $(1 \leq i \leq n)$ denotes a single bit of u. Specifically, x_1 is the leading bit of u, while x_n is the final bit of u. The notation $\bar{x}_i$ denotes the complement of x_i. $0u$ (resp. $1u$) denotes the binary string obtained by prefixing 0 (resp. 1) to u.

For vertex labeling, we use $(0)^m$ (resp. $(1)^m$) to represent a binary string consisting of m consecutive 0s (resp. 1s). If $m = 0$, then $(0)^m$ and $(1)^m$ represent empty strings.

The hypercube Q_n is an n-regular bipartite graph with 2^n vertices, which has a diameter of n. Every vertex in Q_n is assigned a unique n-bit binary string as its label. The formal definition of Q_n is presented below.

Definition 1. *(see [12]) An n-dimensional hypercube Q_n $(n \geq 1)$ is a simple graph consisting of 2^n vertices and $n \cdot 2^{n-1}$ edges, where the vertex set is $V(Q_n) = \{x_n x_{n-1} \cdots x_1 | x_i \in \{0, 1\}$ and $1 \leq i \leq n\}$. Two distinct vertices are adjacent if, and only if, their binary labels differ in exactly one bit.*

The complete Josephus cube CJC_n represents an enhanced hypercube topology, with additional edges that enhance its overall connectivity. Its formal definition is given as follows:

Definition 2. *(see [13]) A complete Josephus cube CJC_n $(n \geq 3)$ has the vertex set $V(CJC_n) = V(Q_n)$ and the edge set $E(CJC_n) = E_h(CJC_n) \cup E_j(CJC_n) \cup E_c(CJC_n)$, where*
(1) $E_h(CJC_n) = \{(x_n \cdots x_{k+1} x_k x_{k-1} \cdots x_2 x_1, x_n \cdots x_{k+1} \bar{x}_k x_{k-1} \cdots x_2 x_1) \mid k \in \{1, 2, \ldots, n\}\}$,
(2) $E_j(CJC_n) = \{(x_n x_{n-1} \cdots x_3 x_2 x_1,\ x_n x_{n-1} \cdots x_3 \bar{x}_2 \bar{x}_1)\}$,
(3) $E_c(CJC_n) = \{(x_n x_{n-1} \cdots x_3 x_2 x_1,\ \bar{x}_n \bar{x}_{n-1} \cdots \bar{x}_3 \bar{x}_2 \bar{x}_1)\}$.

The edges in $E_h(CJC_n), E_j(CJC_n), E_c(CJC_n)$ are called H-edges (Hypercube edges), J-edges (Josephus edges), and C-edges (Complementary edges), respectively. CJC_n is an $(n+2)$-regular graph, as each vertex is incident to one J-edge, one C-edge, and n H-edges in CJC_n. CJC_3 and CJC_4 are illustrated in Figure 1 where H-edges are represented by black solid lines, J-edges by red dashed lines, and C-edges by green dashed lines. Like other hypercube variants, there is another recursive definition for an n-dimensional complete Josephus cube.

Definition 3. *An n-dimensional complete Josephus cube $CJC_n(n \geq 3)$ is defined recursively as follows:*
(a) CJC_3 is shown in Figure 1;
(b) For $n \geq 4$, CJC_n is constructed from two copies of CJC_{n-1}. Let CJC^0_{n-1} (resp. CJC^1_{n-1}) be the graph obtained by prefixing each vertex of one copy of CJC_{n-1} with 0 (resp. 1). Remove all $(n-1)$-dimensional C-edges in CJC^0_{n-1} and CJC^1_{n-1}, then connect each vertex $0x_{n-1}x_{n-2}...x_1 \in V(CJC^0_{n-1})$ with the vertex $1\bar{x}_{n-1}\bar{x}_{n-2}...\bar{x}_1 \in V(CJC^1_{n-1})$ by an n-dimensional C-edge, and connect each vertex $0x_{n-1}x_{n-2}...x_1 \in V(CJC^0_{n-1})$ with the vertex $1x_{n-1}x_{n-2}...x_1 \in V(CJC^1_{n-1})$ by an H-edge.

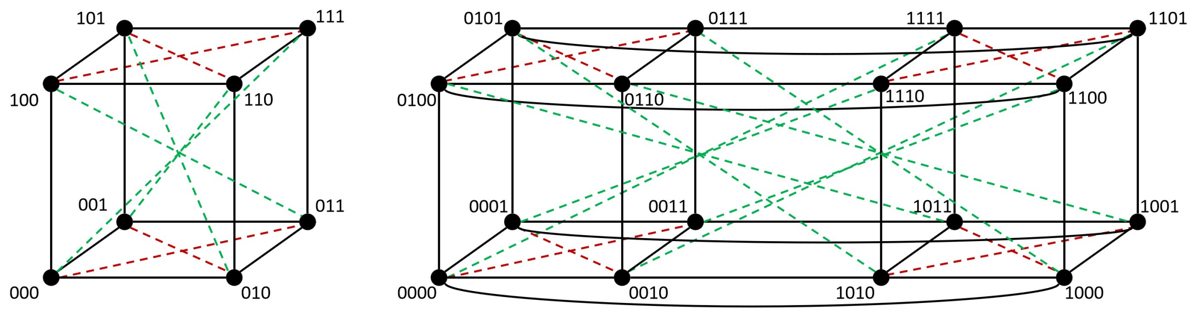

Figure 1. The complete Josephus cubes CJC_3 and CJC_4.

When we construct CJC_n from two copies CJC^0_{n-1} and CJC^1_{n-1} of CJC_{n-1}, the C-edges in CJC^0_{n-1} and CJC^1_{n-1}, called $(n-1)$-dimensional C-edges, are no longer valid within the CJC_n structure. To address this, we remove all such outdated $(n-1)$-dimensional C-edges from both subgraphs. We then re-establish the required connectivity by introducing new n-dimensional C-edges and H-edges.

For example, to construct CJC_4 from two copies of CJC_3, we first create two subgraphs CJC^0_3 and CJC^1_3. For each vertex in CJC^0_3, take 0000 as an instance; we need to remove the edge (0000,0111) (a 3-dimensional C-edge), connect 0000 with 1111 via the edge (0000,1111) (a 4-dimensional C-edge), and link 0000 with 1000 by the edge (0000,1000) (an H-edge).

3. Main results

In this section, we investigate the edge-disjoint cycle embedding of CJC_n for any integer $n \geq 3$. Let $n \geq 3$. A path $\langle u, x, y, v\rangle$ in CJC_n with $(u, x), (y, v) \in E_c(CJC_n)$ and $(x, y) \in E_h(CJC_n)$ is called an F-path. An F-subpath is an F-path that occurs as a subpath of a longer path in CJC_n.

We first introduce a lemma that will be employed in our subsequent analysis.

Lemma 1. *Let R be a Hamiltonian path in $CJC_n(n \geq 3)$ with $r = 2^{n-2}$ F-subpaths containing all C-edges of CJC_n. Then, when constructing CJC_{n+1} from two disjoint copies CJC^0_n and CJC^1_n of CJC_n, the union of the two new paths derived from R covers all vertices of CJC_{n+1}, and the resulting $2r$ F-subpaths contain all C-edges of CJC_{n+1}.*

Proof. Since $CJC^0_n \cong CJC^1_n \cong CJC_n$, there exist Hamiltonian paths R^0 in CJC^0_n and R^1 in CJC^1_n derived from R, such that both R^0 and R^1 contain r F-subpaths. Moreover, all C-edges of CJC^0_n (resp. CJC^1_n) are contained within the r F-subpaths of R^0 (resp. R^1). Let

$$R^0 = \langle 0start(R), \ldots, 0u_1, 0x_1, 0y_1, 0v_1, \ldots, 0u_r, 0x_r, 0y_r, 0v_r, \ldots, 0end(R)\rangle,$$

and

$$R^1 = \langle 1start(R), \ldots, 1u_1, 1x_1, 1y_1, 1v_1, \ldots, 1u_r, 1x_r, 1y_r, 1v_r, \ldots, 1end(R)\rangle,$$

where for $i \in \{0, 1\}$ and $1 \leq j \leq r$, the subsequence $\langle iu_j, ix_j, iy_j, iv_j\rangle$ forms an F-subpath. Recall that the edges (iu_j, ix_j) and (iy_j, iv_j) are n-dimensional C-edges in CJC_n^i. According to Definition 3, when constructing CJC_{n+1} from CJC_n^0 and CJC_n^1, the n-dimensional C-edges (iu_j, ix_j) and (iy_j, iv_j) in each copy are removed, and the $(n+1)$-dimensional C-edges $(iu_j, \bar{i}x_j)$ and $(iy_j, \bar{i}v_j)$ in CJC_{n+1} are added (while all other edges remain unchanged); consequently, the vertex iu_j is not adjacent to ix_j, and iy_j is not adjacent to iv_j in CJC_{n+1}. To obtain paths in CJC_{n+1}, we make some updates as follows:

$$R^{0\text{update}} = \langle 0start(R), \ldots, 0u_1, 1x_1, 1y_1, 0v_1, \ldots, 0u_r, 1x_r, 1y_r, 0v_r, \ldots, 0end(R)\rangle,$$

and

$$R^{1\text{update}} = \langle 1start(R), \ldots, 1u_1, 0x_1, 0y_1, 1v_1, \ldots, 1u_r, 0x_r, 0y_r, 1v_r, \ldots, 1end(R)\rangle.$$

See Figure 2. By Definition 3, since (u_j, x_j) and $(y_j, v_j) \in E_c(CJC_n)$, we have that

$$(0u_j, 1x_j), (1y_j, 0v_j), (1u_j, 0x_j), (0y_j, 1v_j) \in E_c(CJC_{n+1}).$$

It concludes that both $R^{0\text{update}}$ and $R^{1\text{update}}$ are paths of CJC_{n+1}, each containing r F-subpaths. For $i \in \{0, 1\}$ and $1 \leq j \leq r$, each F-subpath $\langle iu_j, \bar{i}x_j, \bar{i}y_j, iv_j\rangle$ has 2 C-edges of CJC_{n+1}. Hence, all $2r$ F-subpaths contain all C-edges of CJC_{n+1}. Since R^0 and R^1 are Hamiltonian paths of CJC_n^0 and CJC_n^1, respectively, we have $V(R^{0\text{update}}) \cup V(R^{1\text{update}}) = V(CJC_{n+1})$ (see Figure 2). □

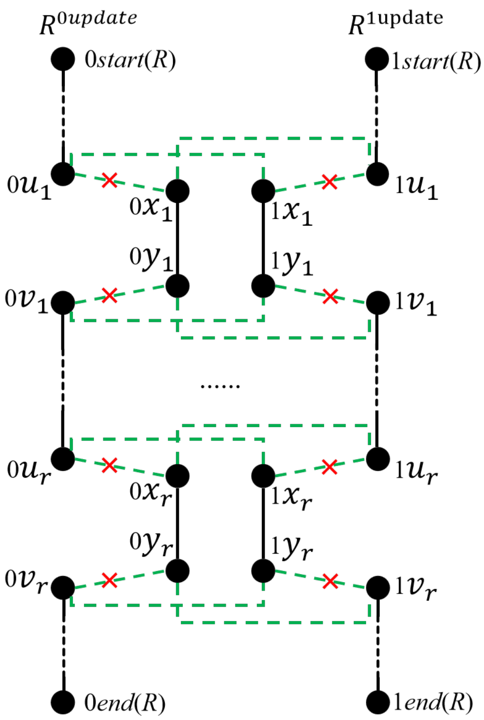

Figure 2. Two new paths $R^{0update}$ and $R^{1update}$ in $CJC_{n+1} (n \geq 3)$ derived from R.

Lemma 2. *There exist two edge-disjoint Hamiltonian paths R and S in CJC_3 such that R contains 2 F-subpaths covering all C-edges of CJC_3, where*

$$start(R) = 000, \quad end(R) = 100,$$
$$start(S) = 011, \quad end(S) = 111.$$

Proof. Two Hamiltonian paths R and S in CJC_3 are constructed as follows:

$$R = \langle 000, 111, 110, 001, 101, 010, 011, 100\rangle,$$

and

$$S = \langle 011, 000, 001, 010, 110, 100, 101, 111\rangle.$$

As shown in Figure 3, R and S are explicitly EDHPs in CJC_3. The two F-subpaths $\langle 000, 111, 110, 001\rangle$ and $\langle 101, 010, 011, 100\rangle$ of path R contain all C-edges of CJC_3, while S contains no C-edges. □

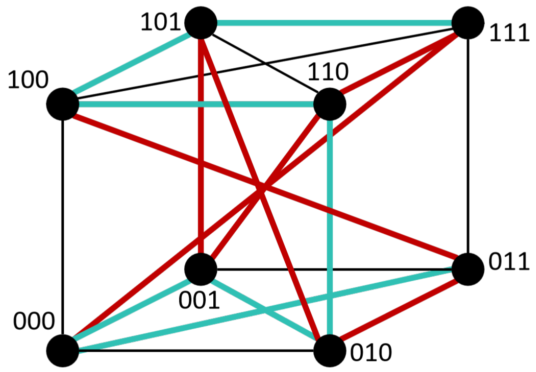

Figure 3. Two EDHPs in CJC_3, where red lines indicate one Hamiltonian path R and green lines indicate the other Hamiltonian path S.

Since $(start(R), end(R)), (start(S), end(S)) \in E(CJC_3)$, R and S can each be closed to form two EDHCs in CJC_3.

Lemma 3. *There exist two edge-disjoint Hamiltonian paths R and S in $CJC_n(n \geq 3)$ such that R contains 2^{n-2} F-subpaths covering all C-edges of CJC_n, where*

$$start(R) = 0(0)^{n-3}00, \quad end(R) = 1(0)^{n-3}00,$$
$$start(S) = 0(0)^{n-3}11, \quad end(S) = 1(0)^{n-3}11.$$

Proof. We use induction on n, the dimension of CJC_n, to prove this lemma. By Lemma 2, the result holds for $n = 3$. Assume the lemma holds for $n \geq 3$, and we consider CJC_{n+1}. According to Definition 3, CJC_{n+1} can be constructed from two disjoint copies CJC_n^0 and CJC_n^1 of CJC_n. By the induction hypothesis, $CJC_n^i (i \in \{0, 1\})$ contains two EDHPs R^i and S^i, such that R^i contains 2^{n-2} F-subpaths, where

$$start(R^i) = i0(0)^{n-3}00, \quad end(R^i) = i1(0)^{n-3}00,$$
$$start(S^i) = i0(0)^{n-3}11, \quad end(S^i) = i1(0)^{n-3}11.$$

First, we consider the paths R^0 and R^1 derived from R. Using the method in Lemma 1, from the paths R^0 and R^1 in CJC_n^0 and CJC_n^1, we obtain two new paths $R^{0update}$ and $R^{1update}$ in CJC_{n+1}, whose union covers all vertices of CJC_{n+1}. Since

$$(end(R^{0update}), end(R^{1update})) \in E(CJC_{n+1}).$$

We define $R = R^{0update} \Longrightarrow R_{rev}^{1update}$, where

$$start(R) = 00(0)^{n-3}00 \quad \text{and} \quad end(R) = 10(0)^{n-3}00.$$

Then, R is one Hamiltonian path in CJC_{n+1}. Again, the combined path R in CJC_{n+1} contains 2^{n-1} F-subpaths covering all C-edges of CJC_{n+1} by Lemma 1.

Next, we turn to the paths S^0 and S^1. During the construction of CJC_{n+1}, only the n-dimensional C-edges in each copy are removed. As S^0 and S^1 contain no such edges, all their edges are preserved in CJC_{n+1}. Since $end(S^0)$ is adjacent to $end(S^1)$ by Definition 2. We now define $S = S^0 \Longrightarrow S_{rev}^1$ where

$$\begin{aligned} start(S) &= 00(0)^{n-3}11, \\ end(S) &= 10(0)^{n-3}11, \\ (start(S), end(S)) &\in E_h(CJC_{n+1}). \end{aligned}$$

Then, S is the other Hamiltonian path in CJC_{n+1} containing no C-edges.

In CJC_n^0 and CJC_n^1, we have

$$E(R^0) \cap E(S^0) = \emptyset \quad \text{and} \quad E(R^1) \cap E(S^1) = \emptyset.$$

During the construction of CJC_{n+1}, S^0 and S^1 remain completely unchanged, while R^0 and R^1 are updated to $R^{0update}$ and $R^{1update}$ without involving any edges from the paths S^0 and S^1. Since

$$\begin{aligned} E(R) &= E(R^{0update}) \cup E(R^{1update}) \cup (end(R^{0update}), end(R^{1update})), \\ E(S) &= E(S^0) \cup E(S^1) \cup (end(S^0), end(S^1)), \end{aligned}$$

we have $E(R) \cap E(S) = \emptyset$. This construction yields two EDHPs R and S in CJC_{n+1} with

$$\begin{aligned} start(R) &= 0(0)^{n-2}00, \quad & end(R) &= 1(0)^{n-2}00, \\ start(S) &= 0(0)^{n-2}11, \quad & end(S) &= 1(0)^{n-2}11. \end{aligned}$$

Thus, the lemma holds for dimension $n+1$, and by induction, it holds for all $n \geq 3$. The construction of two EDHPs is illustrated in Figure 4. $\square$

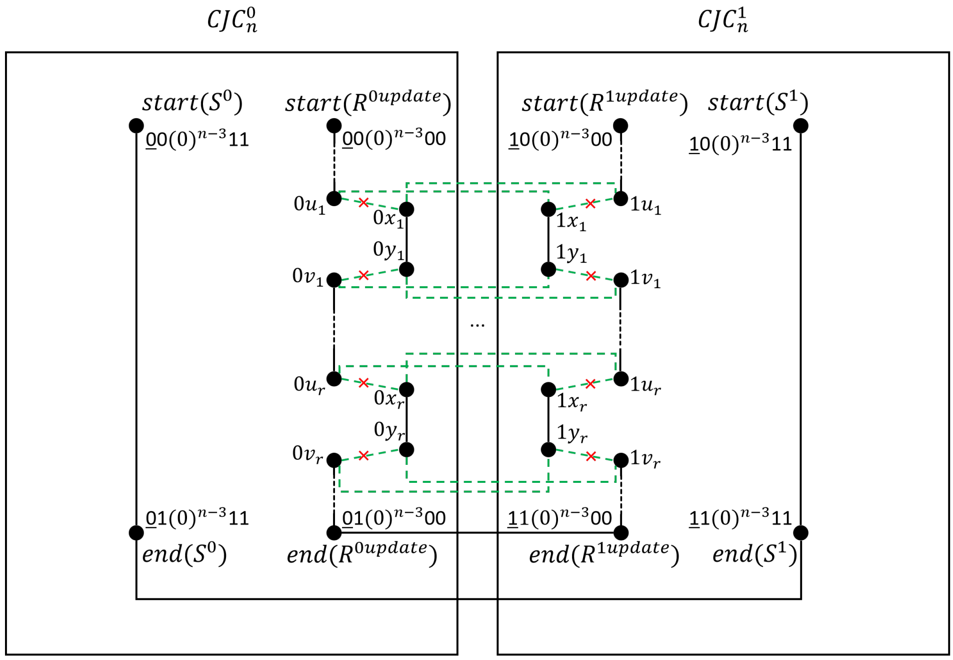

Figure 4. The construction of two EDHPs in CJC_{n+1} with $n \geq 3$.

Since path R contains 2^{n-1} F-subpaths, and these F-subpaths collectively cover all 2^n C-edges of CJC_{n+1}, then the construction of other Hamiltonian paths can proceed without considering the reconstruction of C-edges during the construction of CJC_{n+1}. Figure 5 illustrates the construction process of the two EDHPs in CJC_4.

Based on the proofs of Lemma 2 and 3, we develop a recursive algorithm (see Algorithm 1) for constructing two EDHPs in an n-dimensional complete Josephus cube. The algorithm recursively computes two EDHPs for each subgraph. These four paths are then concatenated into two EDHPs for CJC_n using the method from Lemma 3 (see Algorithms 2 and 3). The algorithms are formally presented below.

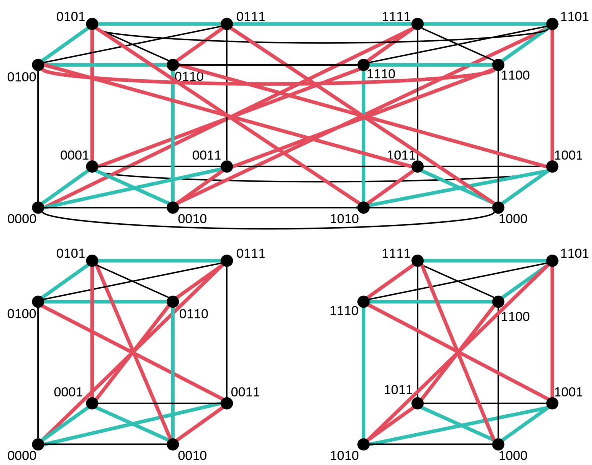

Figure 5. The construction of two EDHPs in CJC_4.

Algorithm 1. Constructing 2 EDHPs (Constr-2HP).

Input: The complete Josephus cube CJC_n of dimension n with $n \geq 3$
Output: Two EDHPs R and S in CJC_n such that

$$start(R) = 0(0)^{n-3}00, \quad end(R) = 1(0)^{n-3}00,$$
$$start(S) = 0(0)^{n-3}11, \quad end(S) = 1(0)^{n-3}11.$$

if $n = 3$ **then**
  $R \leftarrow \langle 000, 111, 110, 001, 101, 010, 011, 100 \rangle$;
  $S \leftarrow \langle 011, 000, 001, 010, 110, 100, 101, 111 \rangle$;
  return R and S such that

$$start(R) = 000, \quad end(R) = 100,$$
$$start(S) = 011, \quad end(S) = 111;$$

else
  call Algorithm *Constr-2HP*(CJC_{n-1}) to compute two EDHPs R' and S' in CJC_{n-1} such that

$$start(R') = 0(0)^{n-4}00, \quad end(R') = 1(0)^{n-4}00,$$
$$start(S') = 0(0)^{n-4}11, \quad end(S') = 1(0)^{n-4}11;$$

  prefix each vertex of R' and S' with 0 to obtain two new paths R^0 and S^0;
  prefix each vertex of R' and S' with 1 to obtain two new paths R^1 and S^1;
  call Algorithm *Concat-2CP*(R^0, R^1, n) to generate path R where

$$start(R) = 0(0)^{n-3}00, \quad end(R) = 1(0)^{n-3}00;$$

  call Algorithm *Concat-2NCP*(S^0, S^1, n) to generate path S where

$$start(S) = 0(0)^{n-3}11, \quad end(S) = 1(0)^{n-3}11;$$

  return R and S such that

$$start(R) = 0(0)^{n-3}00, \quad end(R) = 1(0)^{n-3}00,$$
$$start(S) = 0(0)^{n-3}11, \quad end(S) = 1(0)^{n-3}11;$$

end if

Algorithm 2. Concatenate 2 paths containing C-edges (Concat-2CP).

Input: Dimension n of the complete Josephus cube CJC_n ($n \geq 3$), paths R^0 and R^1
Output: A new path R joining with R^0 and R^1
1: Remove all C-edges of dimension $n-1$ from R^0;
2: Remove all C-edges of dimension $n-1$ from R^1;
3: Connect each vertex in R^0 to a corresponding vertex in R^1 via a C-edge of dimension n to obtain two new paths $R^{0update}$ and $R^{1update}$;
4: $R^{1update} \leftarrow$ reverse $R^{1update}$;
5: $R \leftarrow R^{0update} \Rightarrow R^{1update}$;
6: **return** R.

Algorithm 3. Concatenate 2 paths containing no C-edges (Concat-2NCP).

Input: Dimension n of the complete Josephus cube $CJC_n (n \geq 3)$, paths S^0 in CJC^0_{n-1} and S^1 in CJC^1_{n-1}
Output: A new path S joining with S^0 and S^1
1: $S^1 \leftarrow$ reverse S^1;
2: $S \leftarrow S^0 \Rightarrow S^1$;
3: **return** S.

In Lemma 3, $start(R)$ is adjacent to $end(R)$, and $start(S)$ is adjacent to $end(S)$ according to Definition 2. Hence, there exist two EDHCs in CJC_n ($n \geq 3$). We have the following theorem.

Theorem 1. *There exist two edge-disjoint Hamiltonian cycles in CJC_n for $n \geq 3$.*

Next, we will prove there exist three EDHCs in CJC_n when $n \geq 4$.

Lemma 4. *There exist three edge-disjoint Hamiltonian paths R, S, and T in CJC_4 such that R contains 4 F-subpaths covering all C-edges of CJC_4, where*

$$\begin{aligned} start(R) &= 0000, & end(R) &= 1000, \\ start(S) &= 0011, & end(S) &= 1011, \\ start(T) &= 0001, & end(T) &= 1001. \end{aligned}$$

Proof. We can obtain two EDHPs R and S' from the structure of CJC_4 (illustrated in Figure 5), where

$$R = \langle 0000, 1111, 1110, 0001, 0101, 1010, 1011, 0100, 1100, 0011, 0010, 1101, 1001, 0110, 0111, 1000 \rangle,$$
$$S' = \langle 0011, 0000, 0001, 0010, 0110, 0100, 0101, 0111, 1111, 1101, 1100, 1110, 1010, 1001, 1000, 1011 \rangle.$$

After removing these two EDHPs, we have one C_{12} and one C_4 in CJC_4, where

$$C_{12} = \langle 0000, 0100, 0111, 0011, 0001, 1001, 1011, 1111, 1100, 1000, 1010, 0010, 0000 \rangle,$$
$$C_4 = \langle 0101, 1101, 1110, 0110, 0101 \rangle.$$

To construct three EDHPs, our strategy is to decompose the existing structures (paths and cycles) into open subpaths by removing a carefully selected set E of edges. Then, using the edges from E, we reconnect the open subpaths into new Hamiltonian paths. Here, we set

$$E = \{(1111, 1101), (1100, 1110), (1100, 1111), (1101, 1110)\} \subset E(S') \cup E(C_{12}) \cup E(C_4).$$

Then, we reconnect the open subpaths in S', C_{12}, and C_4 with E, and form two new EDHPs S and T (see Figure 6). Hence, there exist three EDHPs R, S, and T in CJC_4, where

$$R = \langle 0000, 1111, 1110, 0001, 0101, 1010, 1011, 0100, 1100, 0011, 0010, 1101, 1001, 0110, 0111, 1000\rangle,$$
$$S = \langle 0011, 0000, 0001, 0010, 0110, 0100, 0101, 0111, 1111, 1100, 1101, 1110, 1010, 1001, 1000, 1011\rangle,$$
$$T = \langle 0001, 0011, 0111, 0100, 0000, 0010, 1010, 1000, 1100, 1110, 0110, 0101, 1101, 1111, 1011, 1001\rangle.$$

The four subpaths $\langle 0000, 1111, 1110, 0001\rangle$, $\langle 0101, 1010, 1011, 0100\rangle$, $\langle 1100, 0011, 0010, 1101\rangle$, and $\langle 1001, 0110, 0111, 1000\rangle$ in R are F-subpaths covering all C-edges of CJC_4, while S and T contain no C-edges. □

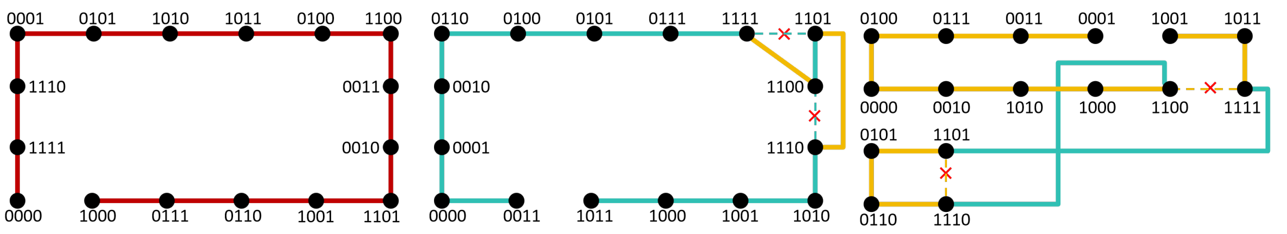

Figure 6. The construction of three EDHPs in CJC_4.

Lemma 5. *There exist three edge-disjoint Hamiltonian paths R, S, and T in $CJC_n (n \geq 4)$ such that R contains 2^{n-2} F-subpaths covering all C-edges of CJC_n, where*

$$start(R) = 0(0)^{n-3}00, \quad end(R) = 1(0)^{n-3}00,$$
$$start(S) = 0(0)^{n-3}11, \quad end(S) = 1(0)^{n-3}11,$$
$$start(T) = 0(0)^{n-3}01, \quad end(T) = 1(0)^{n-3}01.$$

Proof. We proceed by induction on n, the dimension of CJC_n. By Lemma 4, the base case $n = 4$ holds. Assume the lemma is true for $n \geq 4$, and we now consider CJC_{n+1}. By Definition 3, CJC_{n+1} is constructed from two disjoint copies CJC_n^0 and CJC_n^1 of CJC_n. By the induction hypothesis, $CJC_n^i (i \in \{0, 1\})$ contains three EDHPs R^i, S^i, and T^i, such that R^i contains 2^{n-2} F-subpaths, where

$$start(R^i) = i0(0)^{n-3}00, \quad end(R^i) = i1(0)^{n-3}00,$$
$$start(S^i) = i0(0)^{n-3}11, \quad end(S^i) = i1(0)^{n-3}11,$$
$$start(T^i) = i0(0)^{n-3}01, \quad end(T^i) = i1(0)^{n-3}01.$$

First, we consider the paths R^0 and R^1 derived from R. Following the construction in Lemma 3, we obtain two new paths $R^{0update}$ and $R^{1update}$ in CJC_{n+1} and then we define $R = R^{0update} \Longrightarrow R^{1update}_{rev}$, where

$$start(R) = 00(0)^{n-3}00 \quad \text{and} \quad end(R) = 10(0)^{n-3}00.$$

Then, R is one Hamiltonian path in CJC_{n+1} covering all C-edges of CJC_{n+1}.

For the paths S^0 in CJC_n^0 and S^1 in CJC_n^1, following the construction in Lemma 3, we define $S = S^0 \Longrightarrow S^1_{rev}$ where

$$start(S) = 00(0)^{n-3}11 \quad \text{and} \quad end(S) = 10(0)^{n-3}11.$$

Then, S is the other Hamiltonian path in CJC_{n+1} containing no C-edges.

For the paths T^0 in CJC_n^0 and T^1 in CJC_n^1, $end(T^0)$ is adjacent to $end(T^1)$ by Definition 2. As T^0 and T^1 contain no C-edges, all their edges are preserved during the construction of CJC_{n+1}. Similar to S, we define $T = T^0 \Longrightarrow T^1_{rev}$ where

$$start(T) = 00(0)^{n-3}01 \quad \text{and} \quad end(T) = 10(0)^{n-3}01.$$

Then, T is the third Hamiltonian path in CJC_{n+1} containing no C-edges.

In CJC_n^0 and CJC_n^1, we have

$$E(R^0) \cap E(S^0) \cap E(T^0) = \emptyset \quad \text{and} \quad E(R^1) \cap E(S^1) \cap E(T^1) = \emptyset.$$

During the construction of CJC_{n+1}, S^0, S^1, T^0, and T^1 remain completely unchanged, while R^0 and R^1 are updated to $R^{0update}$ and $R^{1update}$ without involving any edges from the paths S^0, S^1, T^0, and T^1. Since

$$\begin{aligned}
E(R) &= E(R^{0update}) \cup E(R^{1update}) \cup (\text{end}(R^{0update}), \text{end}(R^{1update})),\\
E(S) &= E(S^0) \cup E(S^1) \cup (\text{end}(S^0), \text{end}(S^1)),\\
E(T) &= E(T^0) \cup E(T^1) \cup (\text{end}(T^0), \text{end}(T^1)),
\end{aligned}$$

we have $E(R) \cap E(S) \cap E(T) = \emptyset$. This construction yields three EDHPs R, S, and T in CJC_{n+1} with $start(R) = 0(0)^{n-2}00$, $end(R) = 1(0)^{n-2}00$, $start(S) = 0(0)^{n-2}11$, $end(S) = 1(0)^{n-2}11$, $start(T) = 0(0)^{n-2}01$, and $end(T) = 1(0)^{n-2}01$. Thus, the lemma holds for dimension $n + 1$, and by induction, it holds for all $n \geq 4$. The construction of these paths is illustrated in Figure 7. □

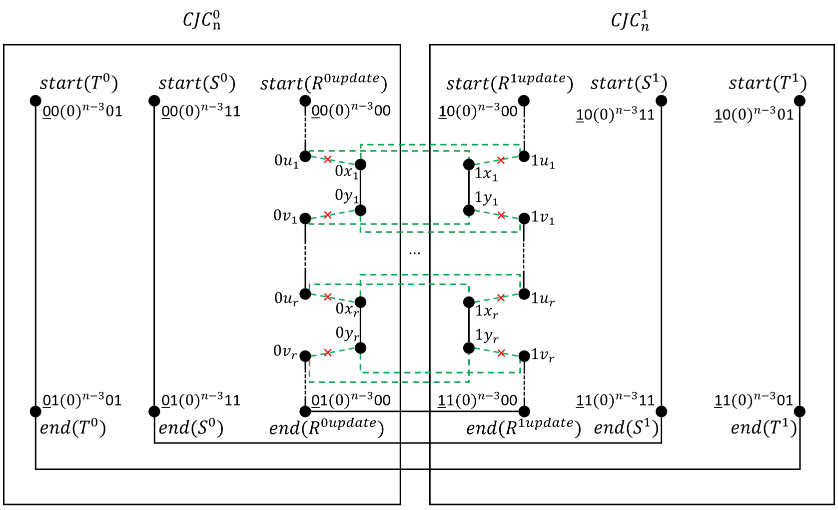

Figure 7. The construction of three EDHPs in CJC_{n+1} with $n \geq 3$.

Based on the proofs of Lemma 4 and Lemma 5, we develop a recursive algorithm (see Algorithm 4) for constructing three EDHPs in an n-dimensional complete Josephus cube. The algorithm is formally presented below.

In Lemma 5, $(start(R), end(R))$, $(start(S), end(S))$, $(start(T), end(T)) \in E(CJC_n)$ $(n \geq 4)$ according to Definition 2. Hence, there exist three EDHCs in CJC_n $(n \geq 4)$. We have the following theorem.

Theorem 2. *There exist three edge-disjoint Hamiltonian cycles in CJC_n for $n \geq 4$.*

Algorithm 4. Constructing 3 EDHPs (Constr-3HP).

Input: The complete Josephus cube CJC_n of dimension n with $n \geq 4$
Output: Three EDHPs R, S, and T in CJC_n such that

$$start(R) = 0(0)^{n-3}00, \quad end(R) = 1(0)^{n-3}00,$$
$$start(S) = 0(0)^{n-3}11, \quad end(S) = 1(0)^{n-3}11,$$
$$start(T) = 0(0)^{n-3}01, \quad end(T) = 1(0)^{n-3}01.$$

if $n = 4$ **then**

$R \leftarrow \langle 0000, 1111, 1110, 0001, 0101, 1010, 1011, 0100, 1100, 0011, 0010, 1101, 1001, 0110, 0111, 1000 \rangle$;

$S \leftarrow \langle 0011, 0000, 0001, 0010, 0110, 0100, 0101, 0111, 1111, 1100, 1101, 1110, 1010, 1001, 1000, 1011 \rangle$;

$T \leftarrow \langle 0001, 0011, 0111, 0100, 0000, 0010, 1010, 1000, 1100, 1110, 0110, 0101, 1101, 1111, 1011, 1001 \rangle$;

return R, S, and T such that

$$\begin{aligned} start(R) &= 0000, & end(R) &= 1000, \\ start(S) &= 0011, & end(S) &= 1011, \\ start(T) &= 0001, & end(T) &= 1001; \end{aligned}$$

else

Call Algorithm *Constr-2HP*(CJC_{n-1}) to compute three EDHPs R', S', and T' in CJC_{n-1} such that

$$\begin{aligned} start(R') &= 0(0)^{n-4}00, & end(R') &= 1(0)^{n-4}00, \\ start(S') &= 0(0)^{n-4}11, & end(S') &= 1(0)^{n-4}11, \\ start(T') &= 0(0)^{n-4}01, & end(T') &= 1(0)^{n-4}01; \end{aligned}$$

Prefix each vertex of R', S', and T' with 0 to obtain three new paths R^0, S^0, and T^0;

Prefix each vertex of R', S', and T' with 1 to obtain three new paths R^1, S^1, and T^1;

Call Algorithm *Concat-2CP*(R^0, R^1, n) to generate path R where

$$start(R) = 0(0)^{n-3}00 \quad \text{and} \quad end(R) = 1(0)^{n-3}00;$$

Call Algorithm *Concat-2NCP*(S^0, S^1, n) to generate path S where

$$start(S) = 0(0)^{n-3}11 \quad \text{and} \quad end(S) = 1(0)^{n-3}11;$$

Call Algorithm *Concat-2NCP*(T^0, T^1, n) to generate path T where

$$start(T) = 0(0)^{n-3}01 \quad \text{and} \quad end(T) = 1(0)^{n-3}01;$$

return R, S, and T such that

$$\begin{aligned} start(R) &= 0(0)^{n-3}00, & end(R) &= 1(0)^{n-3}00, \\ start(S) &= 0(0)^{n-3}11, & end(S) &= 1(0)^{n-3}11, \\ start(T) &= 0(0)^{n-3}01, & end(T) &= 1(0)^{n-3}01; \end{aligned}$$

end if

4. Performance evaluation

In this section, we simulate data broadcasting in complete Josephus cubes (CJC_n) under multiple edge failures. The networks considered in our simulations are CJC_n for $n \in \{3, 4, 5, 6, 7, 8, 9, 10, 11\}$. We use one, two, and three EDHCs as transmission channels, and let F be the set of faulty edges with $1 \leq |F| \leq 10$. We evaluate the fault-tolerant capability by measuring the experimental transmission success rate ($TSR_{experiment}$), defined as the ratio of successful broadcast instances to the total number of generated instances. A broadcast is considered successful if every node in CJC_n can receive the message through at least one of the available EDHCs. For the CJC_n networks, we implemented the data broadcasting simulation using the Java programming language. The simulations were carried out on a Lenovo laptop equipped with a 1.8 GHz Intel(R) Core(TM) i7-8550U CPU, 8 GB RAM, and a Windows 11 operating system.

For each network dimension n, number of Hamiltonian cycles m, and number of faulty edges k where $n \geq 3$, $1 \leq m \leq 3$, and $1 \leq k \leq 10$, 100000 random faulty edge sets $\{f_1, f_2, ..., f_k\}$ are generated as experimental instances. Data broadcasting is performed in parallel via m Hamiltonian cycles. If faulty edges appear in all m Hamiltonian cycles simultaneously, the data transmission will fail. Otherwise, the data broadcasting will succeed as long as at least one Hamiltonian cycle remains fault-free. The primary purpose of the simulations is to systematically investigate the impact of the number of EDHCs on the fault tolerance of data broadcasting in complete Josephus cubes.

For the purpose of further verifying the validity of our simulation experiments, we derive the theoretical transmission success rate (TSR_{theory}) using the closed-form expression, and conduct a side-by-side comparison between the theoretical and simulated results. Since the cycles are edge-disjoint and the faulty edges are selected uniformly at random from the entire edge set, the transmission success probability can be derived analytically using combinatorial probability. Specifically, let $N = (n+2)\times 2^n$ be the total number of edges, $L = 2^n$ be the length of each Hamiltonian cycle, and m be the number of EDHCs used. For a fixed number of faulty edges $|F| = k$, the broadcast succeeds if, and only if, at least one cycle contains no faulty edge. Using inclusion–exclusion, the exact success probability is

$$\mathrm{TSR}_{\mathrm{theory}} = \frac{1}{\binom{N}{k}} \sum_{j=1}^{m} (-1)^{j-1} \binom{m}{j} \binom{N - jL}{k}. \tag{4.1}$$

We compare the experimental simulation results against the theoretical values computed using our derived closed-form expression. The test scenarios cover 9-dimensional, 10-dimensional, and 11-dimensional complete Josephus cube networks, with the number of uniformly random faulty edges k ranging from 1 to 10, and the number of EDHCs $m = 1, 2, 3$. The detailed comparison results are shown in Table 1.

According to Figure 8 and Table 1, we are conscious of the following three phenomena:
(1) The simulation experiments are validated to be highly reliable, as the simulated broadcast success rates ($TSR_{experiment}$) exhibit an excellent match with the theoretical values (TSR_{theory}) calculated by the closed-form expression across all tested scenarios in Table 1. Specifically, the maximum deviation between experimental and theoretical results is less than 0.0037 for all cases, with most scenarios showing deviations well below 0.0020.
(2) The number of EDHCs plays a decisive role in determining the $TSR_{experiment}$ during data

broadcasting in CJC_n networks. Across all tested network sizes from CJC_3 to CJC_{11}, the $TSR_{experiment}$ values consistently follow a clear hierarchy: Three-EDHCs>Two-EDHCs>One-EDHC. This demonstrates that increasing the number of EDHCs directly enhances the network's ability to maintain successful data broadcasting as the number of faulty edges $|F|$ increases.
(3) The size of the CJC_n network also exerts a significant influence on $TSR_{experiment}$ performance. In smaller networks, such as CJC_3 and CJC_4, the $TSR_{experiment}$ values drop sharply with increasing $|F|$. In contrast, larger CJC_n networks (e.g., CJC_9 to CJC_{11}) exhibit more gradual $TSR_{experiment}$ decay. Even at the maximum fault count of $|F| = 10$, larger networks maintain substantially higher $TSR_{experiment}$ values, especially for Three-EDHCs.

Table 1. Comparison of simulated and theoretical broadcast success rates for 9/10/11-dimensional CJC networks.

n	k	One-EDHC		Two-EDHCs		Three-EDHCs	
		$TSR_{experiment}$	TSR_{theory}	$TSR_{experiment}$	TSR_{theory}	$TSR_{experiment}$	TSR_{theory}
9	1	0.8183	0.8182	1.0000	1.0000	1.0000	1.0000
	2	0.6719	0.6694	0.9340	0.9339	1.0000	1.0000
	3	0.5476	0.5476	0.8381	0.8376	0.9634	0.9639
	4	0.4472	0.4479	0.7299	0.7320	0.8940	0.8949
	5	0.3659	0.3664	0.6295	0.6286	0.8051	0.8060
	6	0.2991	0.2996	0.5336	0.5331	0.7090	0.7090
	7	0.2461	0.2450	0.4495	0.4480	0.6118	0.6128
	8	0.2010	0.2004	0.3739	0.3740	0.5221	0.5227
	9	0.1641	0.1638	0.3122	0.3107	0.4416	0.4414
	10	0.1329	0.1340	0.2587	0.2571	0.3692	0.3699
10	1	0.8322	0.8333	1.0000	1.0000	1.0000	1.0000
	2	0.6941	0.6944	0.9449	0.9444	1.0000	1.0000
	3	0.5756	0.5786	0.8619	0.8611	0.9729	0.9722
	4	0.4841	0.4822	0.7665	0.7669	0.9159	0.9166
	5	0.4008	0.4017	0.6742	0.6719	0.8413	0.8417
	6	0.3332	0.3347	0.5834	0.5818	0.7577	0.7567
	7	0.2790	0.2789	0.4990	0.4994	0.6712	0.6692
	8	0.2342	0.2324	0.4295	0.4258	0.5832	0.5842
	9	0.1950	0.1936	0.3621	0.3612	0.5028	0.5049
	10	0.1619	0.1613	0.3065	0.3053	0.4325	0.4329
11	1	0.8444	0.8462	1.0000	1.0000	1.0000	1.0000
	2	0.7166	0.7160	0.9522	0.9527	1.0000	1.0000
	3	0.6071	0.6058	0.8799	0.8798	0.9775	0.9781
	4	0.5128	0.5126	0.7968	0.7955	0.9325	0.9328
	5	0.4366	0.4337	0.7066	0.7084	0.8706	0.8694
	6	0.3657	0.3670	0.6253	0.6239	0.7952	0.7951
	7	0.3096	0.3105	0.5462	0.5448	0.7177	0.7160
	8	0.2637	0.2627	0.4754	0.4726	0.6378	0.6369
	9	0.2224	0.2222	0.4050	0.4080	0.5610	0.5611
	10	0.1860	0.1880	0.3493	0.3508	0.4917	0.4904

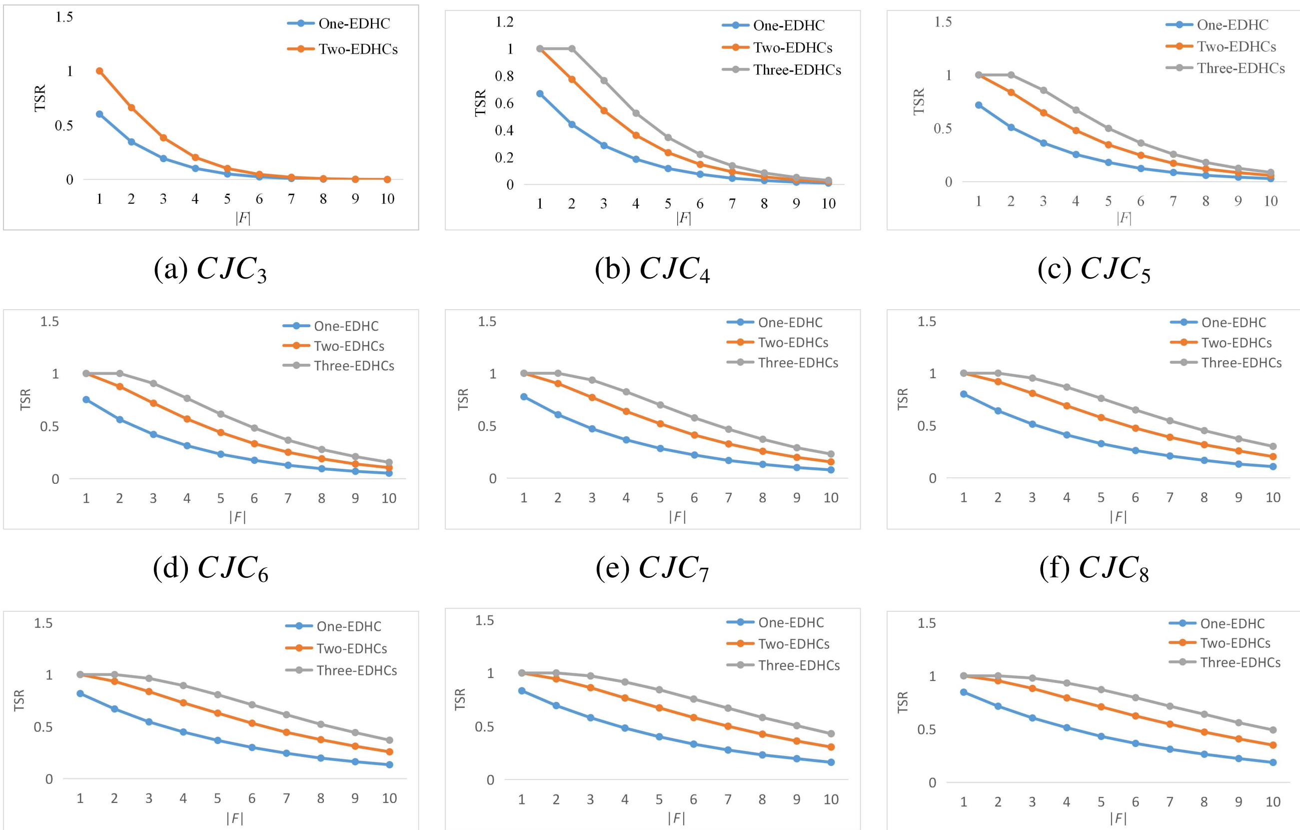

(a) CJC_3 (b) CJC_4 (c) CJC_5

(d) CJC_6 (e) CJC_7 (f) CJC_8

(g) CJC_9 (h) CJC_{10} (i) CJC_{11}

Figure 8. The corresponding trend of the $TSR_{experiment}$ with respect to the scale of CJC_n and the number of faulty edges.

5. Conclusions

EDHCs play a crucial role in enhancing the fault tolerance of interconnection networks, as they provide independent transmission paths that ensure communication continuity even when individual links fail. Additionally, they enable efficient parallel data broadcasting, allowing multiple data streams to be transmitted simultaneously without link interference, thereby improving network throughput and reducing latency. In this work, we establish that CJC_n contains two EDHCs for $n \geq 3$ and three EDHCs for $n \geq 4$. We further conduct experimental evaluations to confirm the practical benefits of these Hamiltonian cycles in data broadcasting scenarios.

Author contributions

Ying Gao: Methodology and Writing—original draft; Lantao You: Conceptualization and Writing-review and editing; Yuejuan Han: Validation and Writing—review and editing. All authors have read and agreed to the published version of the manuscript.

Use of Generative-AI tools declaration

The authors declare they have not used Artificial Intelligence (AI) tools in the creation of this article.

Acknowledgments

This work is supported by the Jiangsu Provincial Science and Technology Deputy Program (No. FZ20251042), the Jiangsu Provincial Industry-University-Research Cooperation Project (No. BY20250620), the Research Platform Project (No. XKYPT-2023-5-P) and Research Project (No. SISO-ZD202202) of Suzhou Industrial Park Institute of Services Outsourcing.

Conflict of interest

The authors declare that they have no conflicts of interest in this work.

References

1. M. M. Bae, B. Bose, Edge disjoint Hamiltonian cycles in k-ary n-cubes and hypercubes, *IEEE Trans. Comput.*, **52** (2003), 1271–1284. https://doi.org/10.1109/TC.2003.1234525
2. R. W. Hung, Embedding two edge-disjoint Hamiltonian cycles into locally twisted cubes, *Theoret. Comput. Sci.*, **412** (2011), 4747–4753. https://doi.org/10.1016/j.tcs.2011.05.004
3. R. W. Hung, C. C. Liao, Constructing two edge-disjoint Hamiltonian cycles and two-equal path cover in augmented cubes, *IAENG Int. J. Comput. Sci.*, **39** (2012), 42–49. Available from: `https://api.semanticscholar.org/CorpusID:18927068`.
4. R. W. Hung, The property of edge-disjoint Hamiltonian cycles in transposition networks and hypercube-like networks, *Discrete Appl. Math.*, **181** (2015), 109–122. https://doi.org/10.1016/j.dam.2014.09.006
5. K. J. Pai, Two edge-disjoint Hamiltonian cycles in shuffle-cubes, *ICS 2024*, 2024, 41–46. https://doi.org/10.1109/ICS64339.2024.00016
6. D. Yang, Z. Xu, Y. Feng, J. Lee, Symmetric property and edge-disjoint Hamiltonian cycles of the spined cube, *Appl. Math. Comput.*, **452** (2023), 128075. https://doi.org/10.1016/j.amc.2023.128075
7. K. J. Pai, R. Y. Wu, S. L. Peng, J. M. Chang, Three edge-disjoint Hamiltonian cycles in crossed cubes with applications to fault-tolerant data broadcasting, *J. Supercomput.*, **79** (2023), 4126–4145. https://doi.org/10.1007/s11227-022-04825-5
8. K. J. Pai, Embedding three edge-disjoint Hamiltonian cycles into locally twisted cubes, *COCOON 2021*, **13025** (2021), 367–374. https://doi.org/10.1007/978-3-030-89543-3_31
9. K. J. Pai, Three edge-disjoint Hamiltonian cycles in folded locally twisted cubes and folded crossed cubes with applications to all-to-all broadcasting, *Mathematics*, **11** (2023), 3384. https://doi.org/10.3390/math11153384
10. H. Lv, T. Wu, Edge-disjoint Hamiltonian cycles of balanced hypercubes, *Inf. Process. Lett.*, **144** (2019), 25–30. https://doi.org/10.1016/j.ipl.2018.12.004

11. S. Liu, Y. Wang, J. Fan, B. Cheng, Edge-disjoint Hamiltonian cycles in balanced hypercubes with applications to fault-tolerant data broadcasting, *Int. J. Found. Comput. Sci.*, **36** (2025), 1–24. https://doi.org/10.1142/S0129054124500047

12. Y. Saad, M. H. Schultz, Topological properties of hypercubes, *IEEE Trans. Comput.*, **37** (1988), 867–872. https://doi.org/10.1109/12.2234

13. P. K. K. Loh, W. Hsu, The Josephus cube: a novel interconnection network, *Parallel Comput.*, **26** (2000), 427–453. https://doi.org/10.1016/S0167-8191(99)00111-8

14. Z. Huang, Y. Yang, M. Zhang, X. Yang, Assessing reliability in Complete Josephus Cube networks via strongly Menger edge-connectivity, *J. Supercomput.*, **81** (2025), 180. https://doi.org/10.1007/s11227-024-06564-1

15. Z. Huang, M. Zhang, C. W. Lee, Connectivity and diagnosability of the complete Josephus cube networks under h-extra fault-tolerant model, *Theoret. Comput. Sci.*, **1020** (2024), 114925. https://doi.org/10.1016/j.tcs.2024.114925

16. Q. He, Y. Wang, J. Fan, B. Cheng, Vertex-independent spanning trees in complete Josephus cubes, *Theoret. Comput. Sci.*, **1025** (2025), 114969. https://doi.org/10.1016/j.tcs.2024.114969

17. Q. He, Y. Wang, J. Fan, B. Cheng, Parallel construction of edge-independent spanning trees in complete Josephus cubes, *J. Supercomput.*, **81** (2025), 334. https://doi.org/10.1007/s11227-024-06784-5

18. S. Liu, Z. Huang, Y. Lv, C. W. Lee, Evaluating the reliability of complete Josephus cubes under extra link fault with the optimal solution of the edge isoperimetric problem, *Theoret. Comput. Sci.*, **1030** (2025), 115064. https://doi.org/10.1016/j.tcs.2025.115064

19. Y. Yang, Z. Huang, M. Zhang, J. Meng, Edge isoperimetric method for link fault tolerance of the complete Josephus cube under five models: a unified approach, *Discrete Appl. Math.*, **378** (2026), 27–36. https://doi.org/10.1016/j.dam.2025.06.043